CLM - P 531

CLM - P 531

UKAEA

Preprint

ANOMALOUS CONDUCTIVITY AND ELECTRON HEATING IN A PLASMA UNSTABLE TO THE TWO-STREAM INSTABILITY

W H M CLARK
S M HAMBERGER

CULHAM LABORATORY
Abingdon Oxfordshire

1978

CLM-P 531

ANOMALOUS CONDUCTIVITY AND ELECTRON HEATING IN A PLASMA UNSTABLE TO THE TWO-STREAM INSTABILITY.

W.H.M. Clark and S.M. Hamberger

Culham Laboratory, Abingdon, Oxon, OX14 3DB, UK
(Euratom/UKAEA Fusion Association)

A B S T R A C T

An experiment to excite the electron-ion two-stream instability in a cylindrical Q-machine plasma column is described. The mechanism for establishing a large pulsed electron drift velocity in the plasma by applying a potential difference between the end electrodes is discussed.

The pulsed current-voltage characteristic of the plasma column and the temporal evolution of the electron density, drift velocity and thermal velocity are measured. In contrast with the behaviour of some computer simulations of the two-stream instability, the plasma exhibits a constant conductivity and the electron thermal velocity increases to values far in excess of the drift velocity. The electrical dissipation is consistent with the increase of the electron thermal energy, both indicating an anomalous conductivity in agreement with the empirical scaling found in earlier experiments on a toroidal discharge.

(Submitted for publication in Plasma Physics)

April 1978

KS

1. INTRODUCTION

In this paper we consider the consequences of applying a steady electric field to a weakly-collisional, fully-ionized plasma column. It is well known that provided the field strength E exceeds the small critical value given by DREICER (1959):

$$E_c \simeq \frac{m v_e(o) \nu_c}{e}$$

(where $v_e(o) = \sqrt{\frac{KT_e}{m}}$ is the initial electron thermal velocity), encounters with the fields of individual ions (denoted by binary collision frequency ν_c) are insufficient to prevent the free acceleration of the bulk of the electron distribution, which in consequence will drift through the background ions with velocity v_d given by:

$$v_d(t) = \frac{Ee}{m} t \qquad \ldots (1)$$

It is equally well known that in reality this acceleration will not continue indefinitely, (as first pointed out by BUDKER, 1956 and BUNEMAN, 1958), owing to the intervention of the electron-ion two-stream instability, since the collective electric fields generated in the plasma will "scatter" the electrons far more effectively than the fields of individual ions.

However the subsequent non-linear behaviour of the system is still far from understood. The thresholds and linear growth rates for the

* Now at: Research School of Physical Sciences, Australian National University, Box 4 P.O., Canberra A.C.T. 2600

instability are readily calculable and well described in the literature (JACKSON 1960 and STRINGER 1964). If the initial ion and electron temperatures T_i and T_e are equal, then the threshold drift velocity is

$$v_d = 1.3\ v_e(o) \qquad \ldots (2)$$

above which the growth rate γ becomes very fast, exceeding the ion plasma frequency ω_{pi}. If $T_e > T_i$ the threshold drift is lower but $\gamma \ll \omega_{pi}$ unless v_d exceeds the threshold (2).

Thus by analogy with E_c, if

$$E \gtrsim E_o = \frac{m v_e(o)\ \omega_{pi}}{e} \qquad \ldots (3)$$

simple argument would suggest that after an initial period of free acceleration (1), threshold (2) will be reached and the collective fields will grow in a timescale $\sim \omega_{pi}^{-1}$ to sufficient amplitude such that both further free acceleration is impeded and the electron drift energy is randomised, the electrons acquiring something resembling a thermal velocity distribution at a higher temperature, effectively quenching the instability since v_d is below the threshold (2). Further acceleration and hence destabilization now recurs, the cycle repeating itself ad nauseam whilst E remains and external losses are insignificant. Thus for a strong field (3) the system will stay close to marginal stability with

$$\overline{v_d(t)} \simeq \overline{v_e(t)} \qquad \ldots (4)$$

where the bar denotes averaging over several such cycles, (i.e. timescales $\gg \gamma^{-1}$) and the mean energy in the fluctuations will remain small (i.e. $\ll nKT$).

If we make a further assumption that the system is conservative such that the increase in electron thermal energy is shared equally

between p degrees of freedom, then from a simple power balance (ignoring energy imparted to the ions, the collective fields, or any external losses) we have

$$E\overline{ev_d} = \frac{d}{dt}\left(\frac{p\overline{mv_e^2}}{2} + \frac{\overline{mv_d^2}}{2} \right) \qquad \ldots (5)$$

Imposing condition (4) results in:

$$v_d(t) \simeq \frac{1}{p+1} \quad \frac{eE}{m} \quad t. \qquad \ldots (6)$$

Comparison with (1) shows that the overall effect of the current-driven turbulence on the average drift velocity is to reduce the free acceleration by a factor $(p+1)$ while leaving the essential runaway behaviour unchanged for timescales $\ll$ external loss timescale, as illustrated in Fig. 1.

This simple model has been inspired by the results of a number of computational experiments using particle simulation codes (e.g. BORIS et al 1970, MORSE and NIELSON 1971). The general behaviour follows the model, i.e. the system remains close to marginal stability, the electron runaway persists and the fluctuation level remains low with a spectral distribution concentrated around those modes with the fastest linear growth rate i.e. wave numbers $k \sim \lambda_D^{-1}$, implying quasilinear processes are important in determining the saturation (HAMASAKI et al 1971).

The macroscopic consequences of the above behaviour are important if we consider the impedance of a plasma column (length ℓ and radius a) when E is derived from a constant external voltage V. Firstly, if the electrons simply undergo free acceleration (1), then the current I is governed by

$$I = \frac{V}{L_o} . t \qquad \ldots (7)$$

where

$$L_o = \frac{m\ell}{ne^2\pi a^2} \qquad \ldots (8)$$

is the inductance due to the inertia of the electrons in the column; (experimentally this is often very small compared to the external circuit inductance). However if $\bar{v}_d$ follows (6) then we can derive an effective collision frequency ν_{eff}, from the momentum equation

$$\frac{d\bar{v}_d}{dt} = \frac{eE}{m} - \nu_{eff} \cdot \bar{v}_d \qquad \ldots (9)$$

by which we obtain

$$\nu_{eff} = \frac{p}{t} \qquad \ldots (10)$$

Thus, for a steady applied field, we have

$$I = \frac{V}{(p + 1)\ L_o} \cdot t \qquad \ldots (11)$$

However, experimental results indicate a plasma behaviour in strong contrast to (10) and (11). In the toroidal experiments of HAMBERGER et al (1968, 1971, 1972, 1975) under conditions where v_d exceeds the threshold (2), the plasma column behaves as a resistance (i.e. ν_{eff} is roughly constant with time), the collective fluctuations remain at a high level and v_e, estimated indirectly by various methods, exceeds v_d by an order of magnitude. The "anomalous" conductivity σ, of the plasma is related to ν_{eff} by:

$$\sigma = \frac{ne^2}{m} \frac{1}{\nu_{eff}} \qquad \ldots (12)$$

HAMBERGER et al found an empirical scaling law for σ in this regime, viz:

$$\frac{\sigma}{4\pi\varepsilon_o} = (0.45 \pm 0.05) \left(\frac{M}{m}\right)^{1/3} \omega_{pe} \qquad \ldots (13)$$

where σ is in S.I. units, M/m is the ion-to-electron mass ratio and

ω_{pe} the electron plasma frequency.

The present work is a further investigation of this phenomenon using a well-understood plasma as a starting point. An experiment has been designed to achieve pulsed electron drifts exceeding threshold (2) in a Q-machine plasma column. Unlike toroidal experiments, the starting conditions are those of a quiescent plasma which is highly reproducible from shot to shot; also the pulse repetition rate ($\sim$ 100 Hz) allows electronic sampling techniques to measure ensemble average quantities easily.

In section 2 the design of the experiment is discussed and sections 3 and 4 describe the behaviour of the electron current under stable and unstable conditions. In section 5 the results of measurements of the temporal evolution of $n(t)$, $v_e(t)$ and $v_d(t)$ are presented followed by a discussion and conclusion in section 6.

2. THE EXPERIMENT

The experiments are conducted in the single-ended Q-machine THESEUS; the tungsten hot plate (2,500 K) produces a thermally ionized potassium plasma column, radius a = 1.3 cm, length ℓ = 80 cm, radially confined by a uniform, axial magnetic field $\underline{B}$ (1 - 4 kG), (MOTLEY, 1975). The hot plate is earthed and the column terminated by an electrically isolated, cold, plane, tantalum disc. The plasma column is inside a cylindrical, concentric, copper waveguide, radius b = 2.6 cm, which is connected to earth close to the hot plate. Over the range of densities used in the experiment ($10^9 - 10^{10}$ cm^{-3}), the axial variation of density is within 1% and the electron mean free path for collisions between neutrals and electrons is much greater than the length of the column. The plasma parameters are always such that the following ordering holds:

$$\omega_{ce} >> \omega_{pe} >> \omega_{pi} >> \omega_{ci} \qquad \ldots (14)$$

where ω_{ce} and ω_{ci} are the electron and ion cyclotron frequencies and ω_{pe}, ω_{pi} the corresponding plasma frequencies.

The object of the experiment is to simulate as closely as possible conditions pertaining to the electron-ion two-stream instability in infinite, collisionless, homogeneous plasma. In order to do this in a single-ended Q-machine plasma, careful consideration must be given to the relevant timescales. In particular:

a) If the accelerating field is such that condition (3) holds and the duration of the current pulse is a few ion plasma periods, then the electron drift will exceed the threshold (2) in a timescale $\lesssim \omega_{pi}$, allowing the effects of the two-stream instability to develop whilst avoiding confusion due to other current-driven instabilities with $\gamma << \omega_{pi}$ which have been observed in Q-machine plasmas, (e.g. HENDEL and YAMADA, 1974). Over the range of densities used in the experiment E_o varies from 7 to 20 V m^{-1}.

b) The timescale of the instability must be sufficiently short so as to allow the turbulence to develop before energy and/or particles are lost from the system by conduction along field lines to the electrodes thus forming some new mascroscopic equilibrium. This loss timescale is $\sim \ell/v_e$. Thus we require:

$$\omega_{pi}^{-1} << \ell/v_e \qquad \ldots (15)$$

The initial value of v_e corresponds to 3 μs; this puts a lower limit of 10^9 cm^{-3} on the density suitable for the experiment.

c) The effects of binary collisions on the electron dynamics should be negligible during the growth of the fluctuations. This requirement puts an upper limit of 10^{10} cm^{-3} on the density.

It is important also to give careful consideration to the manner in which a uniform electron drift can be established within the bulk of the plasma column merely by applying a voltage pulse between the end electrodes, when in the absence of collisions (i.e. prior to the development of turbulence) there can be no quasi-stationary electrostatic potential gradient along the column. This is discussed in the next section.

3. ESTABLISHMENT OF THE PULSED ELECTRON CURRENT

Pulsed currents through the plasma column are produced using the circuit shown in Fig. 2. Positive going pulses with rise time τ_r = 20 ns and duration ~ 2 μs are applied via an isolating capacitor to the cold plate, the repetition rate being adjusted to allow the plasma column to return to its original equilibrium condition. (This depends on the amplitude and duration of the pulses and lies between 100 and 1000 Hz). The coaxial cable and the cylindrical waveguide together provide a low inductance (~ 0.5 μH) return path for the current when compared with L_o in (8) which is ~ 12 μH.

In normal usage the equilibrium of a single-ended Q-machine is established by allowing the cold plate to float at a negative potential with respect to the plasma column, thus absorbing all the ions and reflecting nearly all the electrons. When a positive potential step V, is applied to the cold plate the electrons are absorbed and the ions are reflected. The rise time τ_r, of the potential is such that:

$$\omega_{pi}^{-1} >> \tau_r >> \omega_{pe}^{-1} \qquad \ldots (16)$$

Because the plate potential varies slowly on the electron time-scale ω_{pe}^{-1}, those electrons adjacent to the plate readily screen it from the plasma column. (The ion dynamics can be

ignored since the ion equilibrium changes on a timescale M/m times longer than the electron transit time along the column). However the absorption of electrons by the anode (cold plate) produces an electron density rarefaction front which moves towards the cathode (hot plate). For reasons which will become clear, the propagation of this perturbation can be expressed in terms of low frequency ($\omega \sim \tau_r^{-1} << \omega_{pe}$) electron plasma wave eigenmodes of the column which can be adequately described by linearised cold fluid theory.

For simplicity we consider a strongly magnetised ($\omega_{ce} >> \omega_{pe}$), cold, homogenous plasma column, completely filling a cylindrical waveguide, radius a. Thus the dispersion relation for the lowest order (0,0) eigenmode is: (TRIVELPIECE and GOULD, 1959)

$$\left(\frac{\omega}{\omega_{pe}}\right)^2 = \frac{(ka)^2}{(ka)^2 + (2.4)^2} \qquad \ldots (17)$$

which holds provided:

$$\omega >> \omega_{pi}$$

and

$$v_e << \omega/\kappa << \text{velocity of light, c.}$$

The eigenfunction for the potential of this mode is,

$$\phi(r,z,t) = \phi_o J_o\left(\frac{2.4\ r}{a}\right) e^{i(kz - \omega t)} \qquad \ldots (18)$$

with similar expressions for the perturbed electron density and velocity. For low frequencies ($\omega_{pi} << \omega << \omega_{pe}$) and long wavelengths ($ka << 2.4$), such eigenfunctions are almost non-dispersive, having approximately the same phase and group velocities

$$\frac{\partial\omega}{\partial k} \simeq \frac{\omega}{k} \equiv u \simeq \frac{\omega_{pe} a}{2.4} \qquad \ldots (19)$$

so that the front will propogate along the column almost undistorted, accelerating electrons towards the anode as it passes. It is convenient to regard the column as a loss-less transmission line with characteristic

impedance, (CLARK 1976)

$$Z_o = \frac{1}{3.27\ ae}\sqrt{\frac{m}{n\ e_o}} \qquad \ldots (20)$$

and characteristic velocity u. Typically, $Z_o = 700\ \Omega$ and $u = 2 \times 10^9$ cm s^{-1} for $n = 5 \times 10^9$ cm^{-3}.

Notice that the cold fluid equations may be linearised provided the potential front is small compared with the electron kinetic energy in the inertial frame of the front, i.e. provided

$$\phi_o << \frac{mu^2}{e} \sim 600\ V.$$

The equivalent electrical circuit for the initial transient response is shown in Fig. 3 where V_o is the open-circuit pulse generator voltage, and Z_c represents the effective impedance of the cathode sheath. (Since the timescale for reflection of the ions by the anode is comparatively long we shall neglect the potential drop at the anode sheath during the initial transient).

To estimate a value for Z_c we use a simple but appropriate sheath model. Provided the cathode has sufficient thermionic emission so that there is a large reservoir of electrons, the sheath appears to be space-charge limited (see below). Since, for perveance K, we have $I = KV^{3/2}$, then $Z_c = V/I = K^{-2/3}\ I^{-1/3}$. Z_c depends weakly on I so that for typical experimental parameters, it has a roughly constant value $\sim 70\ \Omega$. Hence the transmission line is mismatched at each end with reflection coefficients,

$$\rho_a = -\left(\frac{Z_o - R}{Z_o + R}\right) \sim -\ 0.9 \text{ at the anode and}$$

$$\rho_c = -\left(\frac{Z_o - Z_c}{Z_o + Z_c}\right) \sim -\ 0.8 \text{ at the cathode.}$$

According to this model the initial potential front should propagate back and forth along the column due to reflections at each end thereby increasing the current in a series of steps. The experimentally obtained oscillogram in Fig. 4(a) confirms that this does indeed occur, the steps being separated in time by $\Delta t = 2\ell/u$ (where u is the value obtained from dispersion measurements rather than equation (19)). Fig. 4(b) shows the signal received by a capacitively coupled probe midway along the column; (this detects a signal $\propto d\phi/dt$).

For timescales $>> 2\ell/u$, (typically $t >> 40$ ns), the electrons in the column can be considered as having been uniformly accelerated. Thus the maximum current (in the absence of plasma resistance) is given by $V_o/(R + Z_c)$ and the risetime determined by the electron inertial inductance L_o in (8).

For $V_o \lesssim 10$ V i.e. below instability threshold, the experimentally measured values of u and Z_o both agree within a factor of two with the estimates based on the simply theory given above, the difference being attributed to the more complicated boundary conditions of the experiment.

Figure 5 shows typical 2 μs duration current pulses I(t) for various applied voltages V. In general for $V \lesssim 5$ volts it is possible to draw steady currents of 20 - 30 μs duration, but for $V \gtrsim 60$ volts, I(t) decays rapidly after 3 - 4 μs even if the applied voltage pulse is of 20 - 30 μs duration.

The behaviour of the current is not affected by the magnetic field in the working range 1 - 4 kG, nor by the hot-plate temperature provided this exceeds some well-defined value (typically 2500 K) which is rather hotter than the usual Q-machine operation ($\sim$ 2000 K). Detailed current measurements (Fig. 7) for $V < 5$ volts (where no

instability occurs and the above model applies), allow the sheath perveance to be determined quantitatively over a wide range of densities. The current behaviour varies slightly with conditions but is covered by the empirical formula,

$$I = KV^{1.6 \pm 0.3} \qquad \ldots (21)$$

where we may call K the perveance, which is proportional to the density as shown in Fig. 6, (the density is determined from the dispersion of electron plasma waves, CLARK 1978).

The values of K are consistent with a space-charge limited sheath of thickness d i.e.

$$K = \frac{4\varepsilon_o}{9} \left(\frac{2e}{m}\right)^{\frac{1}{2}} \frac{\pi a^2}{d^2} \qquad \ldots (22)$$

with d about 5 Debye lengths as might be expected.

4. BEHAVIOUR OF THE CURRENT UNDER UNSTABLE CONDITIONS

When V > 5 volts the behaviour of the current changes and can no longer be explained by the above simple theory for a collisionless column. The dependence of V on I, measured at t = 1 μs, i.e. when the drift conditions are well established, is shown in Fig. 7.

There is a critical current I_c, above which the plasma condition clearly changes. Above this critical current large potential fluctuations are detected by probes over a wide range of frequencies, $\sim \omega_{pi} \rightarrow \omega_{pe}$. These appear at about t > 0.4 - 0.5 μs when the current decreases somewhat (see Fig. 5), and the column exhibits a significant resistance, i.e. a considerably increased voltage is required to increase the current correspondingly (Fig. 7).

Figure 8 shows that the critical current is proportional to the electron density. The solid line corresponds to the threshold (2).

In order to estimate σ for the turbulent plasma from the measured V - I characteristic we assume the following:

a) the sheath drop is unaffected by the presence of the turbulence and hence is determined by (21) and

b) the electric field and current density are axially uniform.

Thus at t = 1 μs

$$E \simeq \frac{V - (I/K)^{2/3}}{\ell} \qquad \ldots (23)$$

hence we calculate,

$$\sigma = \frac{I}{E \pi a^2} \qquad \ldots (24)$$

The variation of σ with I (and the corresponding value of E) for various densities is shown in Fig. 9. The conductivity falls rapidly around I_c and then decreases slowly at higher currents.

Figure 10 shows the variation of the column conductance,

$$\frac{1}{R} = \frac{I}{V - (I/K)^{2/3}}$$

with column length, indicating that (b) is not an accurate assumption although it should be remembered that shortening the column length affects the timescale criterion (15); further discussion is given in the last section.

Finally Fig. 11 shows the dependence of the limiting values of σ at high currents on density. Compared with these values are:

a) the 'classical' conductivity (SPITZER, 1962) for an electron temperature T_e = 2,500 K (≃ 0.2 eV), viz:

$$\sigma = 0.0153 \frac{T_e^{3/2}}{\log \Lambda} \text{ mho m}^{-1} \qquad \ldots (25)$$

b) the 'anomalous' conductivity calculated from the empirical scaling (13).

5. TEMPORAL EVOLUTION OF PLASMA PARAMETERS FROM TIME-RESOLVED MEASUREMENTS OF THE DISPERSION OF ELECTRON PLASMA WAVES

Making direct spatial and temporal measurements of n, v_d and v_e is very difficult. However information can be deduced from the time-resolved measurement of the dispersion of electron plasma waves in the column. Details of the technique are presented in an accompanying paper (CLARK, 1978), here we shall consider the relevant experimental results.

Briefly, the dispersion relation for long wavelength ($ka \lesssim 1$) electron plasma waves can be measured instantaneously, in the presence of turbulent fluctuations, at different times during the pulse. A consistent analysis of the dispersion curves for wave propagating parallel and anti-parallel to the electron drift enables estimates to be made of the first few velocity moments of the electron distribution function f(v), of velocities parallel to B, averaged over scale lengths $\sim$ 1 cm. In particular, the technique is sensitive to changes in v_d which are greater than $v_e(o)$.

The interferometer measurements show that after some initial transient, duration $\sim 0.2 - 0.4$ μs, (CLARK, 1978), the electron drift is axially uniform. This initial transient (which occurs when $I > I_c$) is more complicated than the simple propagating potential ramp discussed in section 4. It is associated with an overshoot of the current pulse (Fig. 5) and the anomalous conductivity. Further discussion will be left to the next section.

Figure 12 shows the evolution of the first five velocity moments (referred to the electron rest frame) during the interval:

$$0.4 \leqslant t \leqslant 0.9 \quad \mu s$$

for $E = 25\ V\ m^{-1}$ estimated from (23), where

$$\left.\begin{aligned} v_d &= \frac{1}{n}\int_{-\infty}^{+\infty} v\, f(v)\, dv \\ v_e^2 &= \frac{1}{n}\int_{-\infty}^{+\infty} (v - v_d)^2\, f(v)\, dv \\ v_a^3 &= \frac{1}{n}\int_{-\infty}^{+\infty} (v - v_d)^3\, f(v)\, dv \\ v_b^4 &= \frac{1}{n}\int_{-\infty}^{+\infty} (v - v_d)^4\, f(v)\, dv \end{aligned}\right\} \quad \ldots (26)$$

These data exhibit the following general features.

a) During the current pulse the electron density remains more or less constant and equal to the initial density n_o.

b) The drift velocity remains more or less constant and the product,

$$I = n\, e v_d\, \pi a^2 \quad \ldots (27)$$

is consistent with the current measured at the anode.

c) The thermal velocity rapidly exceeds the drift and continues to increase implying substantial electron 'heating'.

d) Despite a large uncertainty in the estimate of v_a it is definitely negative for $t > 0$, i.e. in the ion rest frame v_a has the <u>opposite</u> sign to v_d. Thus in the electron rest frame $f(v - v_d)$ is asymmetric (as is also the wave dispersion when viewed from the electron rest frame). This suggests that in velocity-space the electron velocities are preferentially scattered towards the direction of the ion drift as shown schematically in Fig. 13.

Figure 14 shows the evolution of n, v_d and v_e during the interval

$$0.2 < t < 2.0 \quad \mu s$$

for different applied E at a density $n_o = 6 \times 10^9$ cm^{-3}.

The behaviour of $v_e(t)$ clearly shows how energy losses become important. Generally for larger E, v_e reaches its maximum, v_{emax}, in a shorter time τ. The electron energy confinement time is $\sim \tau$, thus the relation between v_{emax} and τ (see Fig. 17) indicates a confinement time $\propto \ell/v_e$, cf (15). $\frac{1}{2} m v_{emax}^2$ is $\sim eE\ell$, hence the electron heating appears to be spectacular, e.g. from 0.2 eV to $\sim$ 60 eV for large values of E.

It is interesting to compare the increase in electron thermal energies with the electrical dissipation. In particular we may estimate ν_{eff} from the rate of increase of v_e for $v_e < v_{emax}$ by the following assumptions.

Power dissipated per unit volume = $n e v_d E$. For a steady drift, if all of the dissipation goes into increasing v_e parallel to E then

$$n e v_d E = \frac{d}{dt} (\tfrac{1}{2} n m v_e^2)$$

so that, from (9):

$$\nu_{eff} = \frac{1}{2 v_d^2} \frac{d}{dt} (v_e^2) \approx \frac{1}{2 v_d^2} \frac{\Delta(v_e^2)}{\Delta t} \qquad \ldots (28)$$

In Fig. 15, $\Delta(v_e^2)/v_d^2$ is plotted against Δt for the results shown in Fig. 14 indicating $\nu_{eff} \sim 7 \times 10^6$ s^{-1}. The corresponding estimates of σ using (12) are consistent with those values obtained from the V - I charactersitic of the column at t = 1 μs, as shown in Fig. 16; (σ is scaled with ω_{pe} to compare with scaling (13), v_d with $v_e(o)$ and the corresponding estimate of E with E_o evaluated from (3)). This consistency between the electrical dissipation and the observed

electron heating is found over a wide range of densities.

6. DISCUSSION AND CONCLUSIONS

It is clear that, of the two contrasting models of plasma behaviour in an external electric field, the results of this experiment are in accord with that of constant conductivity rather than a modified runaway behaviour (6). In particular we should emphasize the following points.

a) The electron acceleration is not limited by the external circuitry in that the rise time of the current under stable conditions is determined by the electron inertia.

b) The theoretically predicted threshold for the electron-ion two-stream instability is clearly observed, (the assumption that the drift velocity is proportional to the current is confirmed by plasma wave dispersion measurements).

c) Both electrical and wave dispersion measurements consistently show that for steady applied electric field the electron drift velocity becomes constant while the thermal velocity increases, substantially exceeding the drift velocity before thermal conduction losses from the ends of the column become significant.

d) Estimates of the conductivity are in all cases at least an order of magnitude lower than the classical value (25) and within a factor of two of the empirical scaling (13).

When the plasma is unstable, the drift velocity transient, the non-uniformity of the electric field after the transient and the current overshoot can be understood qualitatively as follows. When a large voltage ($\gtrsim$ 30 V) is applied to the anode, a potential ramp begins to propagate at velocity u, as described in section 4. The electrons close to the anode will experience a transient field,

$$E = \frac{V}{u\tau_r}$$

before this has propagated along the column. If $V/u\tau_r >> E_o$, the plasma close to the anode will quickly go unstable. Consequently the collisionless theory for the ramp propagation is no longer applicable; the resulting ν_{eff} between those ions and electrons close to the anode, will cause the ramp to steepen, preventing most of it from reaching the cathode. (The front part, where $\phi < E_o\ u\tau_r$, will continue to propagate at velocity u). The establishment of the main part of the potential gradient along the column will now be by a diffusive process rather than a wave propagation process. Consequently the electron drift front diffuses along the column comparatively slowly. As it does so the effective column resistance increases causing the anode current, after an initial fast rise, to fall until the drift is axially uniform throughout the column. However, since the turbulence has begun at different times along the column, the electric field driving the current at a time when the drift is axially uniform (i.e. $t \sim 1\ \mu s$) may itself be axially non-uniform. This process is shown schematically in Fig. 18.

In general all the results, except those relating to the transient phase which are due to the linear geometry used, are consistent with those found in the early work on toroidal discharges by Hamberger et al discussed in section 1.

Concerning other work in this field, results from recent experiments performed in a toroidal geometry appear to be contradictory. HIROSE and SKARSGARD (1976) claim to have observed electron runaway (6) with p = 3 degrees of freedom. However, in their experiment the external circuit inductance $L >> L_o$, so that the raw data is subject

to a large correction, unlike that (e.g. Fig. 12) in this work. GENTLE et al (1977) have observed a constant conductivity and plasma behaviour in general agreement with the results of this work.

As to why the level of turbulence should remain high after v_e has exceeded v_d, in this experiment it is clear that this cannot be explained by the electron current channel breaking up into filaments (HAMBERGER and SHARP 1973) since for such an electromagnetic process the scale length, $c/\omega_{pe} >> a$, the column radius. A possible explanation is furnished by the results of a recent computer simulation (DEGROOT et al 1977). It appears that a resistance can be maintained in a collisionless plasma by the formation of ion density spikes ($\Delta n_i \sim n_o$) and large potential jumps ($e\Delta\phi > \kappa T_e$). The formation of these "double layer" structures has been observed in a magnetic field-free plasma by QUON and WONG, (1976). Clearly in order to see if such a mechanism is present in this experiment, detailed data is required on the potential fluctuations observed when the plasma is unstable, which will be reported in a later publication.

ACKNOWLEDGEMENT

During this work, one of us (W.H.M. Clark) was a member of the Department of Engineering Science, Oxford University, on attachment to Culham Laboratory.

REFERENCES

BORIS, J.P., DAWSON, J.M., ORENS, J.H. and ROBERTS, K.V., (1970) Phys. Rev. Lett. 25, 706.

BUDKER, G.I., (1956) Atom. Energ. 5, 9 (Trans. Sov. Atom. Energ. 1 673 (1956)).

BUNEMAN, O., (1958) Phys. Rev. Lett. 1, 8.

CLARK, W.H.M., (1976) D. Phil. Thesis, Oxford University (unpublished).

CLARK, W.H.M., (1978) Plasma Physics, Accompanying paper, (CLM-P532).

DEGROOT, J.S., BARNES, C., WALSTEAD, A.E. and BUNEMAN O., (1977) Phys. Rev. Lett. 38, 1283.

DREICER, H., (1959) Phys. Rev. 115, 238.

GENTLE, K.W., LEIFESTE, G.T. and RICHARDSON, R., (1977) Procs. Third Int. Congress Waves & Instabilities in Plasmas, Ecole Polytechnique, Paris.

HAMBERGER, S.M. and FRIEDMAN, M., (1968) Phys. Rev. Lett. 21, 674.

HAMBERGER, S.M., JANCARIK, J., SHARP, L.E. and ALDCROFT, D.A., (1971) Plasma Physics and Controlled Nuclear Fusion Research, II, IAEA, Vienna.

HAMBERGER, S.M. and JANCARIK, J., (1972) Physics Fluids, 15, 825.

HAMBERGER, S.M. and SHARP, L.E., (1973) Bull. Amer. Phys. Soc. 18, 1312.

HAMBERGER, S.M., (1975) Procs. Second Int. Congress Waves and Instabilities in Plasmas, Innsbruck (Also Culham Report CLM-P 426).

HAMASAKI, S., DAVIDSON, R.C. and KRALL, N.A., (1971) Physics Fluids, 14, 2385.

HENDEL, H.W. and YAMADA, M., (1974) Phys. Rev. Lett. 33, 1076.

HIROSE, A. and SKARSGARD, H.M., (1976) Phys. Rev. Lett. 36, 252.

JACKSON, J.D., (1960) J. Nucl. Energy, Part C: Plasma Physics, 1, 171.

MORSE, R.L. and NIELSON, C.W., (1971) Phys. Rev. Lett. 26, 3.

MOTLEY, R.W., (1975) Q-machines, Academic Press, New York.

QUON, B.H. and WONG, A.Y., (1976) Phys. Rev. Lett. 37, 1393.

SPITZER, L., (1962) Physics of Fully Ionised Gases, p.139, Interscience, New York.

STRINGER, T.E., (1964) Plasma Physics, 6, 267.

TRIVELPIECE, A.W. and GOULD, R.W., (1959) J. Appl. Phys. 30, 1784.

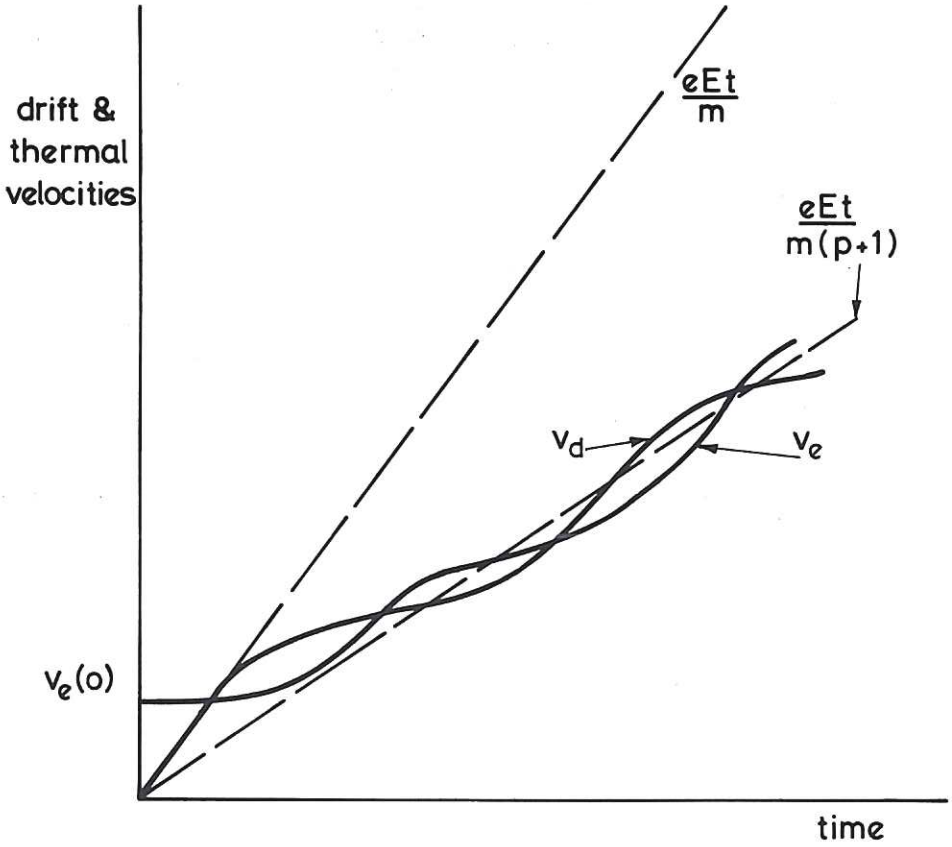

Fig.1 Temporal response of a collisionless plasma to an applied electric field according to the simple model (see text).

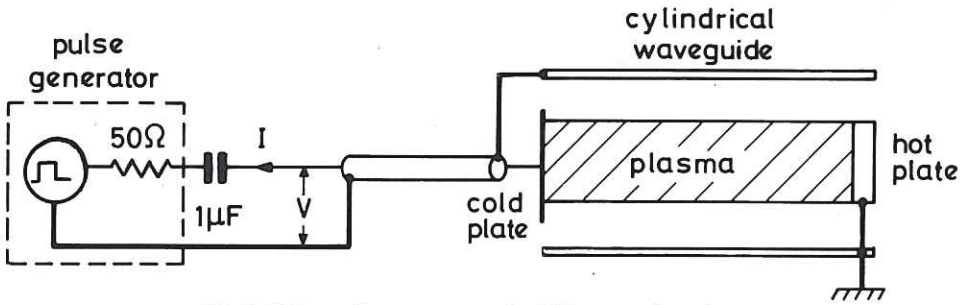

Fig.2 Schematic arrangement of the experiment.

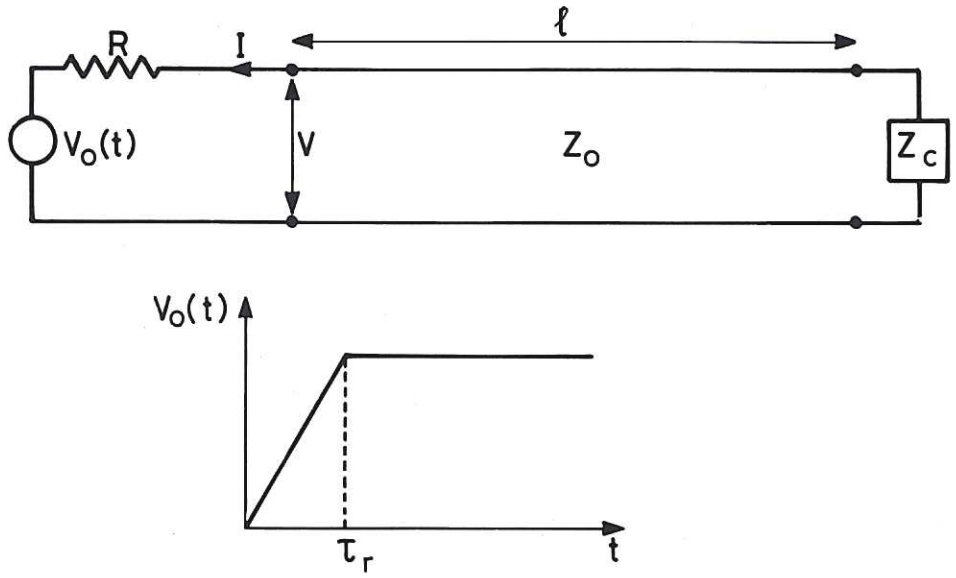

CLM-P 531

Fig.3 Equivalent circuit for the initial transient response.

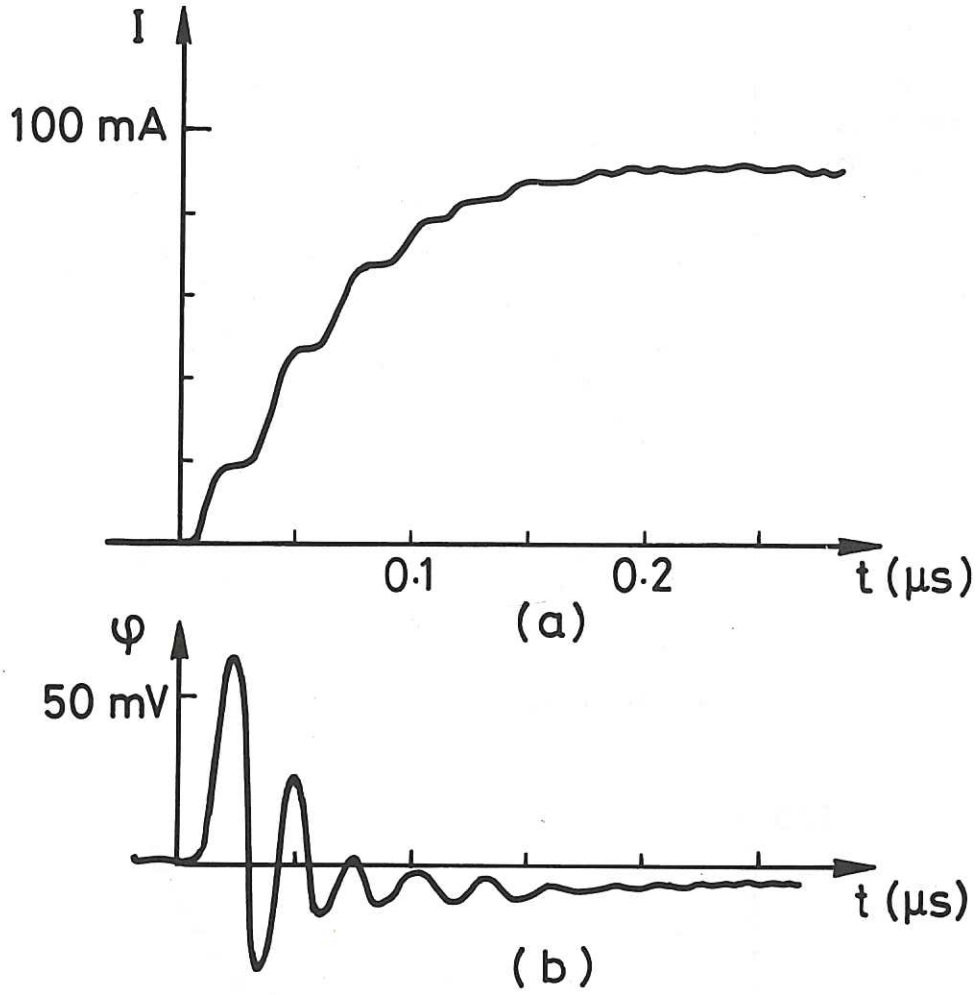

Fig.4 (a) Electron current measured at the anode for V_0 = 10 volts, n = 5 x 10^9 cm^{-3}.
(b) Signal received from a capacitatively-coupled probe midway along the column.

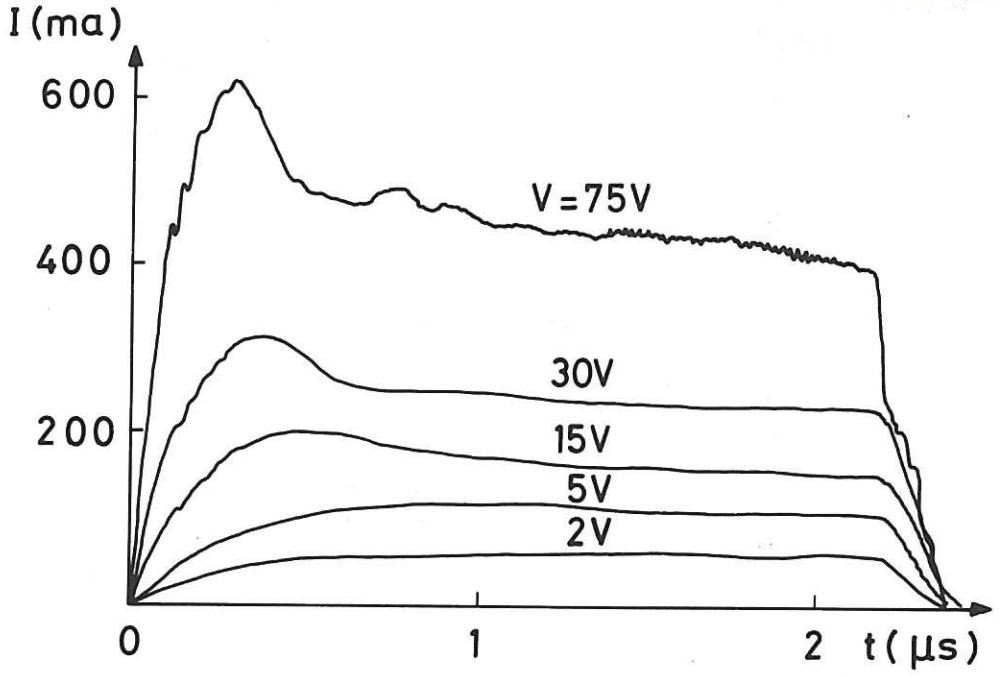

Fig.5 Electron current at the anode for different applied voltage V; n = 6 x 10^9 cm^{-3}.

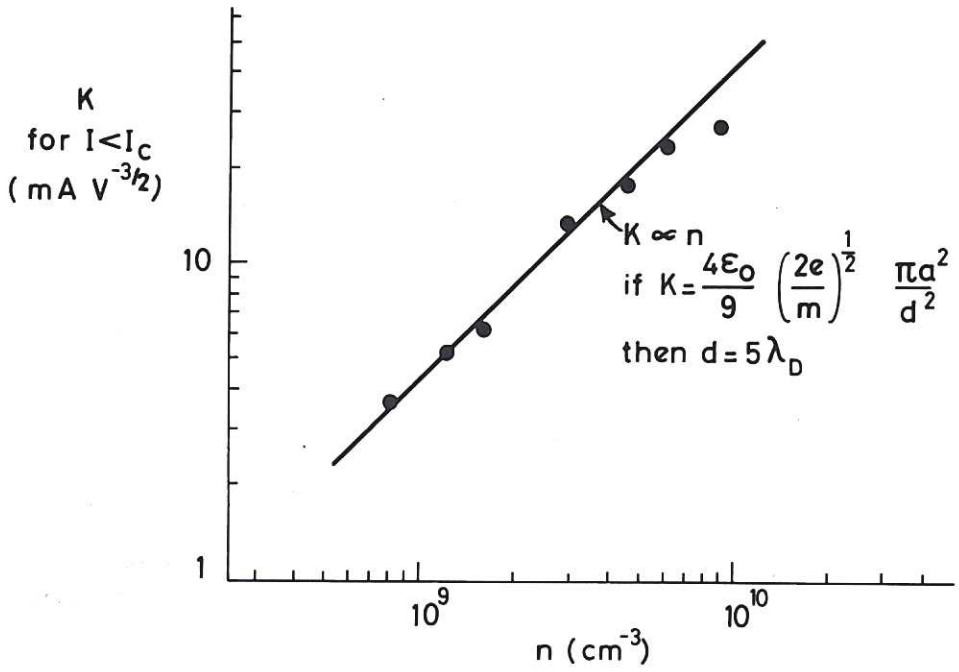

Fig.6 Variation of the perveance K, with density n.

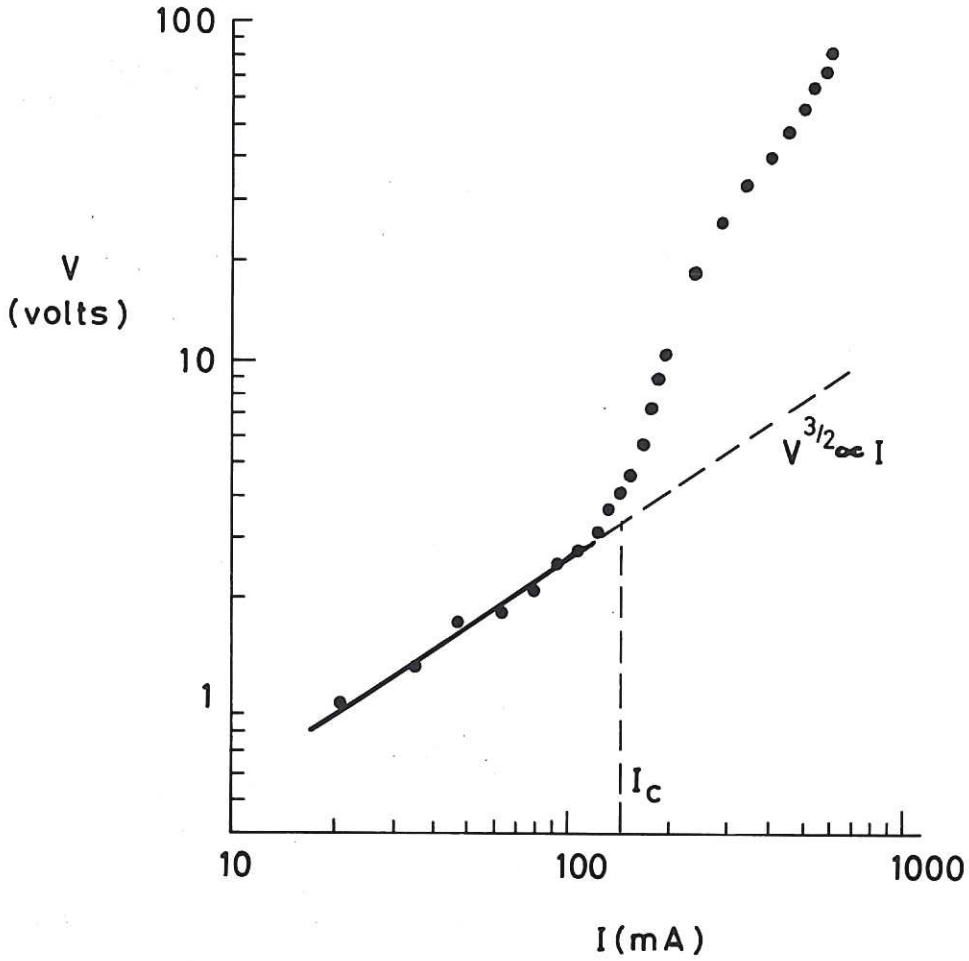

Fig.7 The pulsed voltage-current relationship measured at t = 1 μs for n = 6 x 10^9 cm^{-3}.

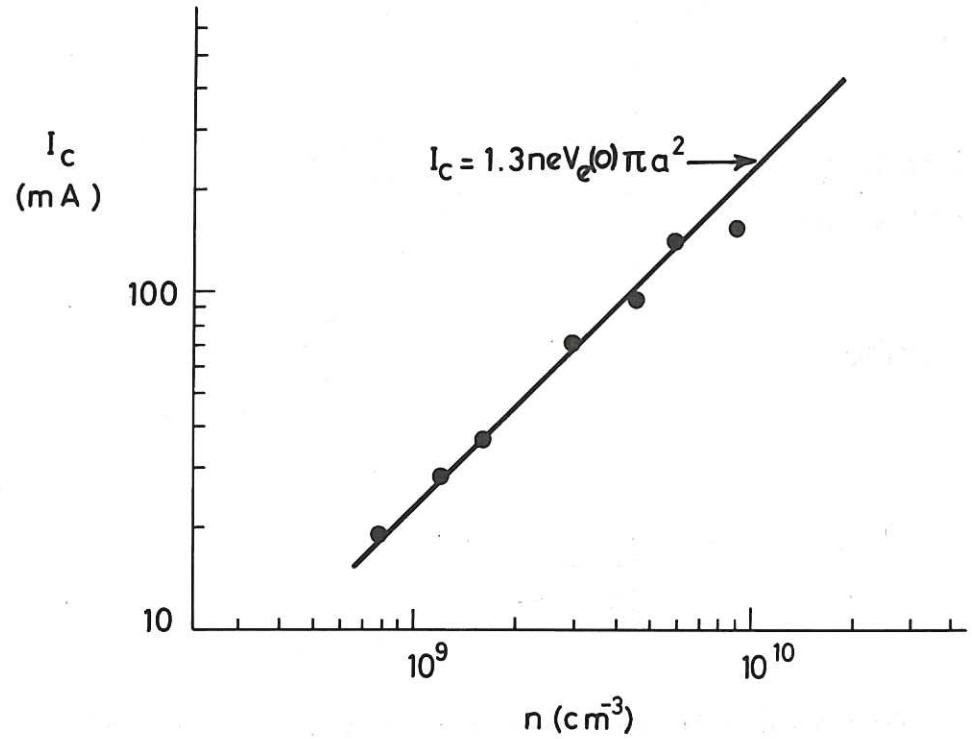

Fig.8 Variation of the critical current I_c with density n.

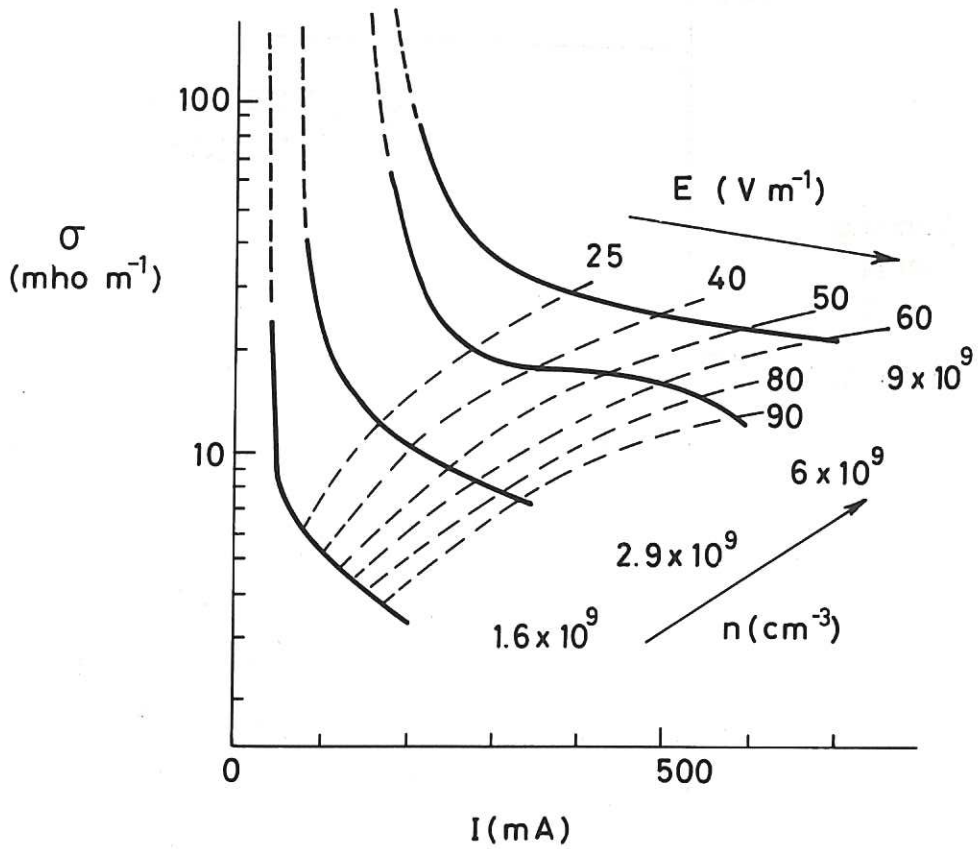

Fig.9 Variation of the plasma conductivity σ computed from the V–I characteristic at 1 μs, with current I and density n.

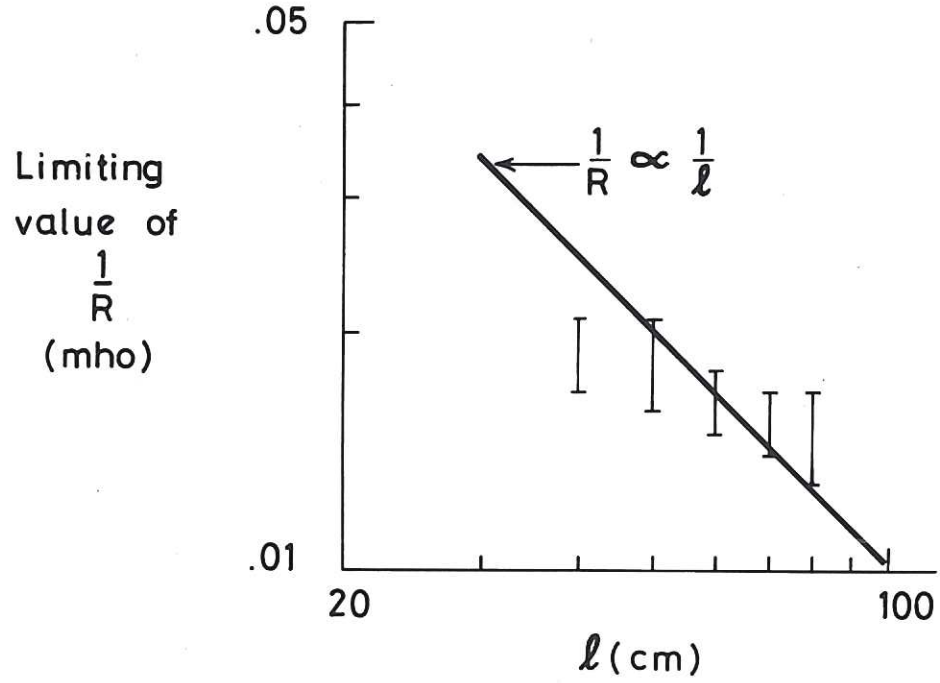

Fig.10 Variation of the column conductance 1/R, at 1 μs with column length ℓ.

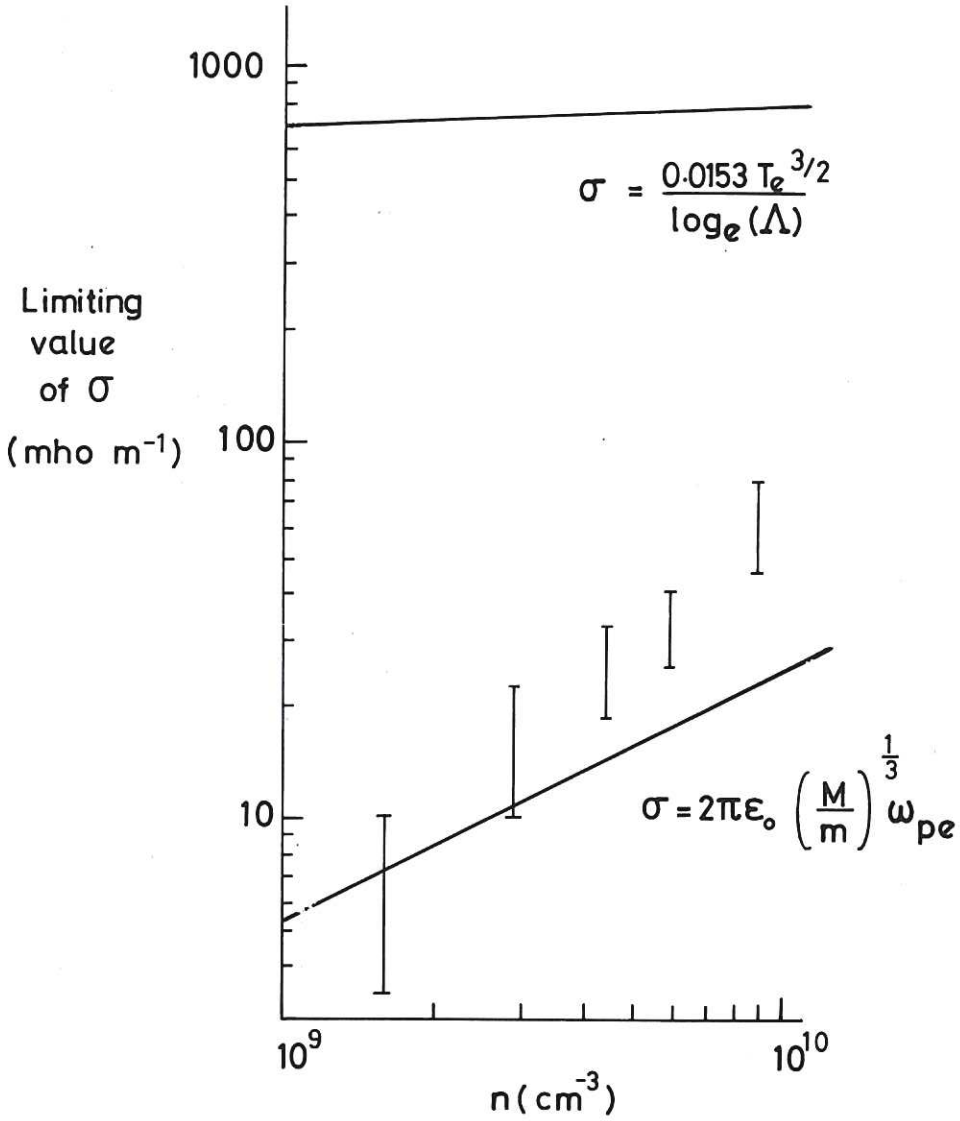

CLM-P 531

Fig.11 The limiting values of σ at 1 μs compared with the classical value (25) and the scaling law (13).

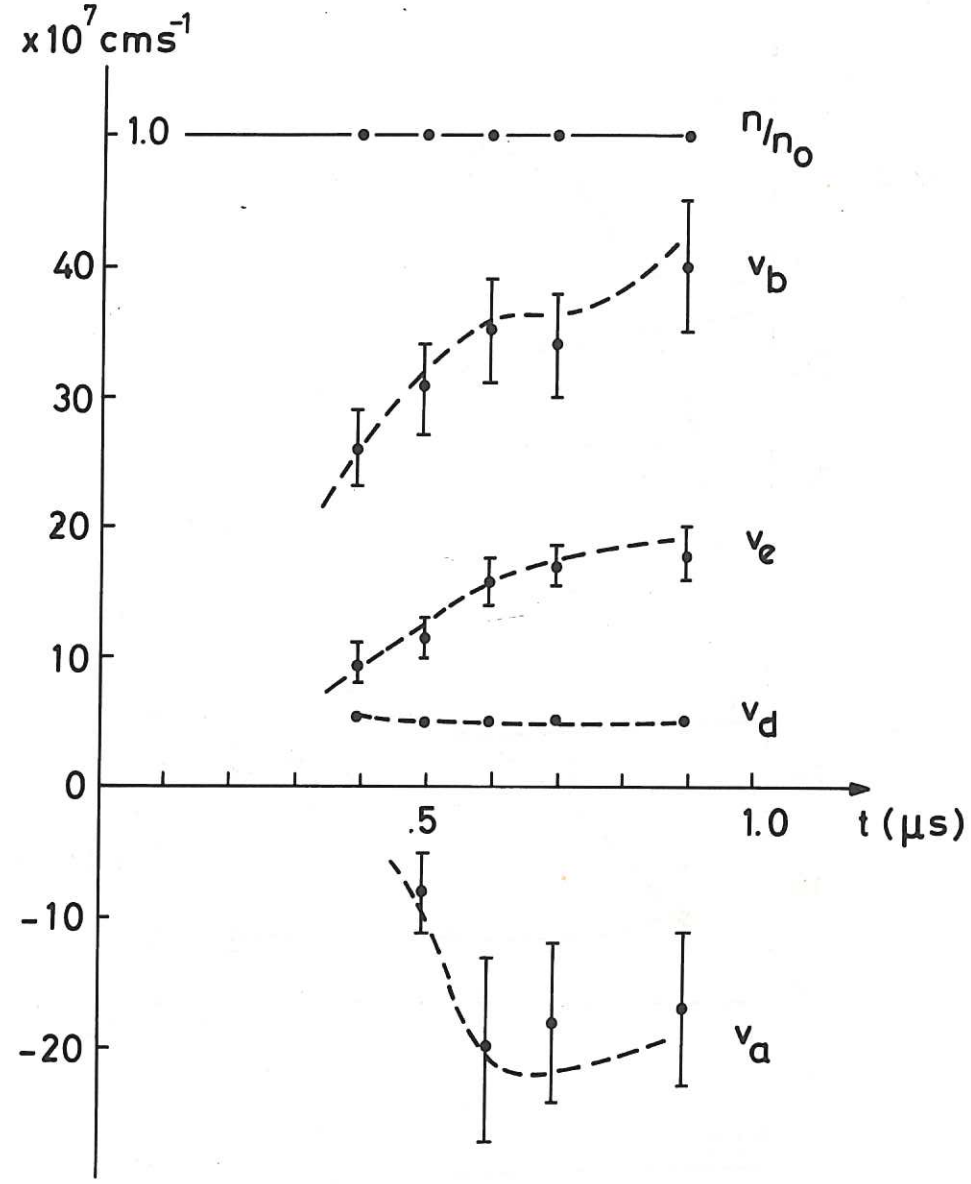

Fig.12 Evolution of the first five velocity moments (see text) for an applied electric field = 25 V m^{-1}, where the density at t = 0 : $n_o = 6 \times 10^9$ cm^{-3}.

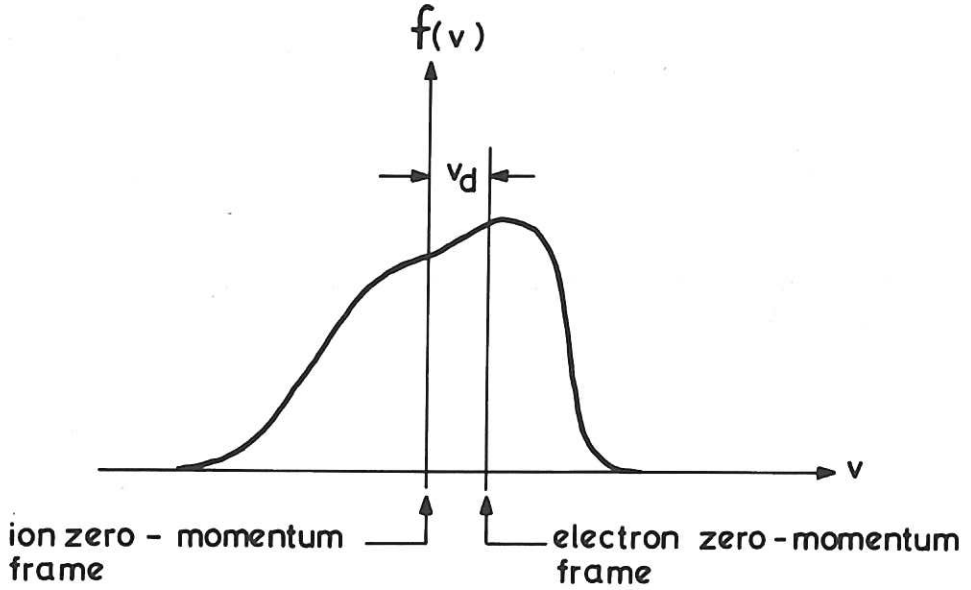

CLM-P 531

Fig.13 Schematic shape of the electron distribution function when v_a has the opposite sign to v_d.

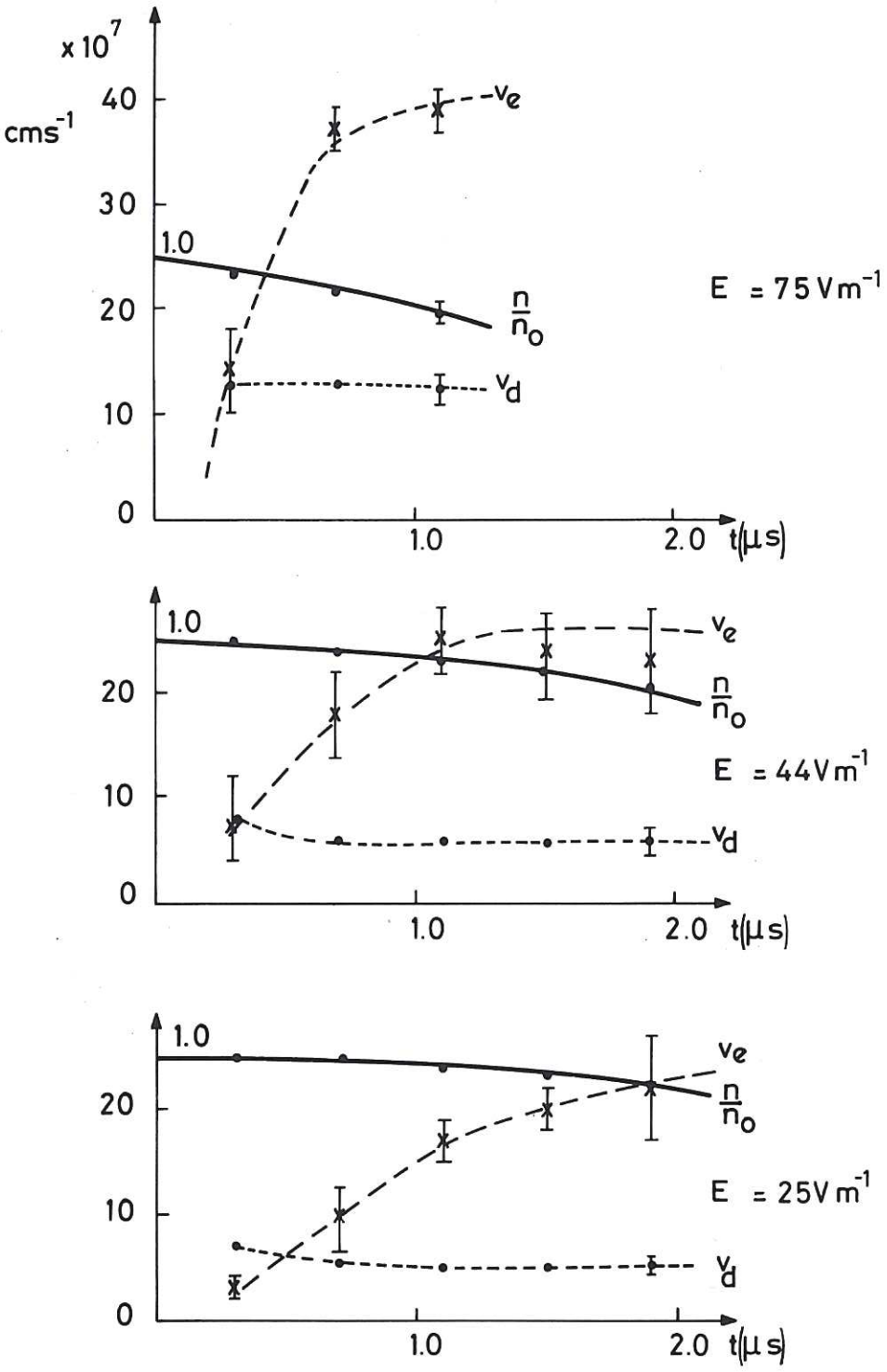

Fig.14 Evolution of the first three velocity moments for different applied electric field E, $n_o = 6 \times 10^9$ cm^{-3}.

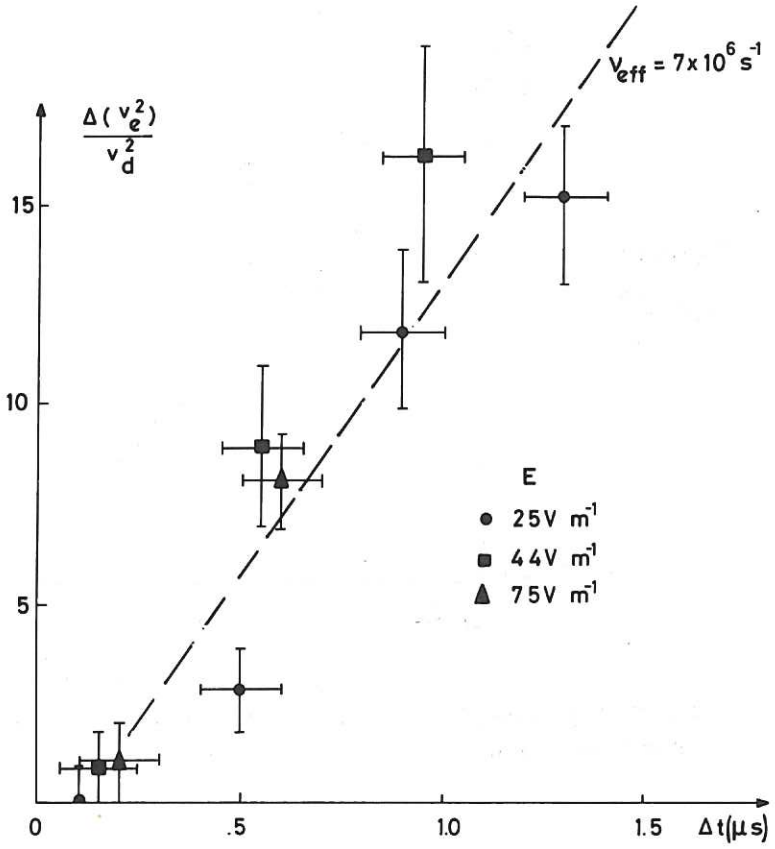

Fig.15 Estimation of ν_{eff} from the electron heating rate.

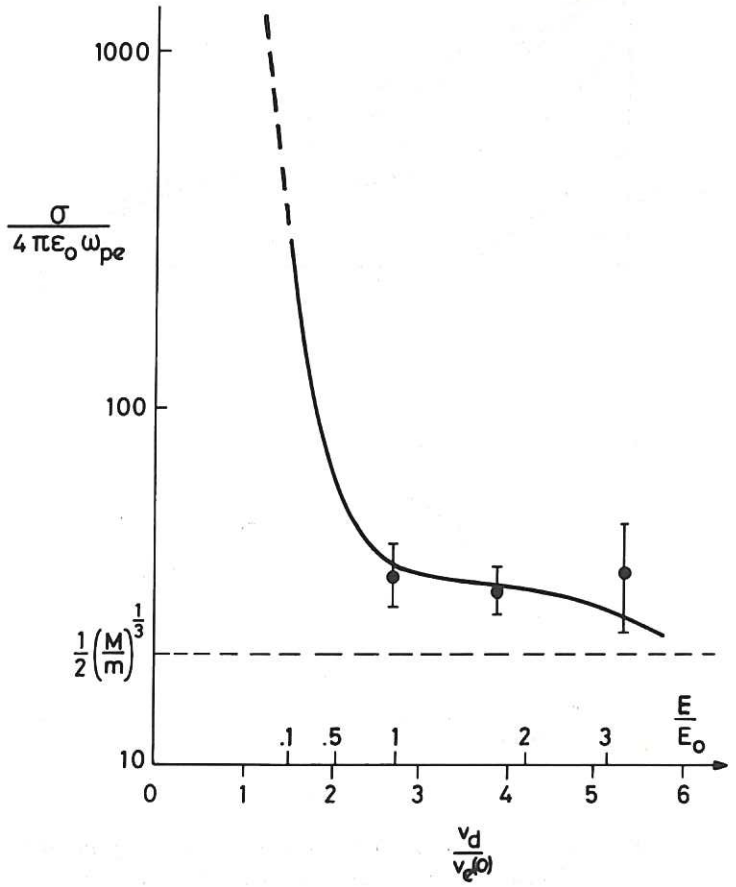

CLM-P 531

Fig.16 Comparison of estimates of conductivity σ, from the measured V–I characteristic at 1 μs (solid line) and the measurement of ν_{eff} (points).

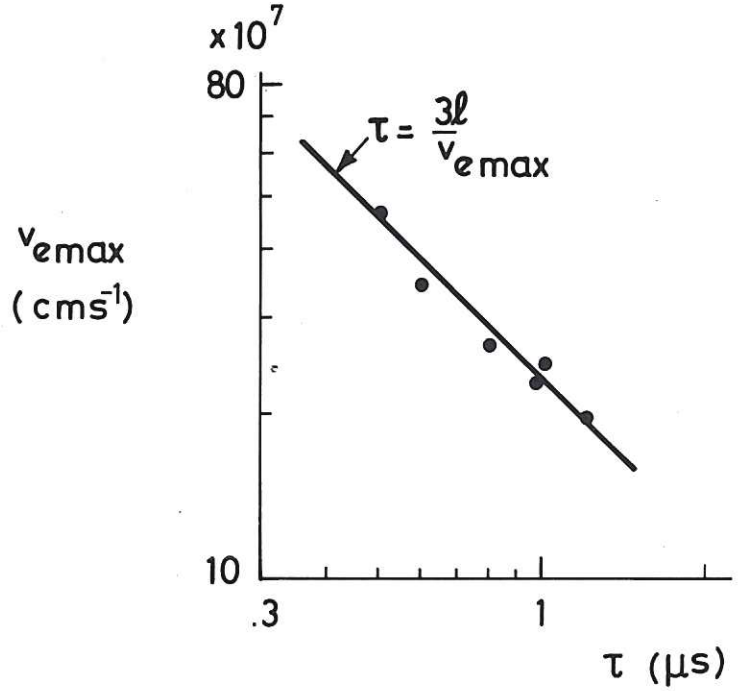

Fig.17 Relation between the maximum value of v_e and the time τ, taken to attain this.

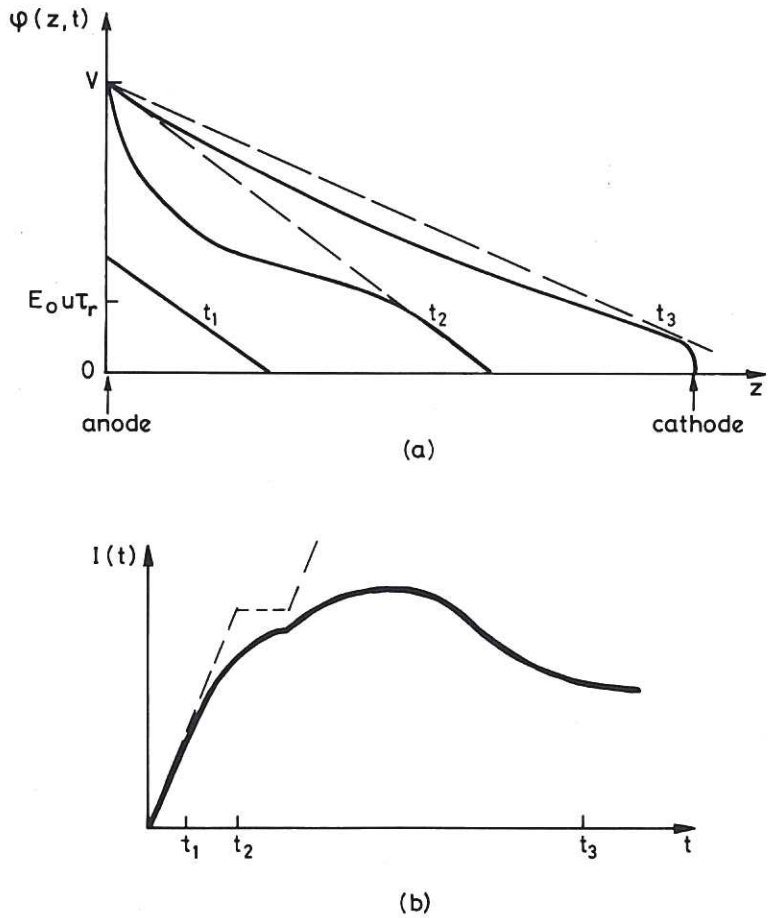

Fig.18 Schematic evolution of (a) the potential along the column $\phi(z,t)$ and (b) the electron current at the anode I(t), when $V \gg E_o u \tau_r$.